

Deformations of reinforced concrete

Autor(en): **Johnson, Arne I.**

Objektyp: **Article**

Zeitschrift: **IABSE publications = Mémoires AIPC = IVBH Abhandlungen**

Band (Jahr): **11 (1951)**

PDF erstellt am: **21.09.2024**

Persistenter Link: <https://doi.org/10.5169/seals-11435>

Nutzungsbedingungen

Die ETH-Bibliothek ist Anbieterin der digitalisierten Zeitschriften. Sie besitzt keine Urheberrechte an den Inhalten der Zeitschriften. Die Rechte liegen in der Regel bei den Herausgebern.

Die auf der Plattform e-periodica veröffentlichten Dokumente stehen für nicht-kommerzielle Zwecke in Lehre und Forschung sowie für die private Nutzung frei zur Verfügung. Einzelne Dateien oder Ausdrucke aus diesem Angebot können zusammen mit diesen Nutzungsbedingungen und den korrekten Herkunftsbezeichnungen weitergegeben werden.

Das Veröffentlichen von Bildern in Print- und Online-Publikationen ist nur mit vorheriger Genehmigung der Rechteinhaber erlaubt. Die systematische Speicherung von Teilen des elektronischen Angebots auf anderen Servern bedarf ebenfalls des schriftlichen Einverständnisses der Rechteinhaber.

Haftungsausschluss

Alle Angaben erfolgen ohne Gewähr für Vollständigkeit oder Richtigkeit. Es wird keine Haftung übernommen für Schäden durch die Verwendung von Informationen aus diesem Online-Angebot oder durch das Fehlen von Informationen. Dies gilt auch für Inhalte Dritter, die über dieses Angebot zugänglich sind.

Deformations of Reinforced Concrete

Formänderungen des Eisenbetons

Déformations du béton armé

ARNE I. JOHNSON, Civil Engineer, Division of Building Statics and Structural Engineering,
Royal Institute of Technology, Stockholm

The deformations of reinforced concrete structures will be studied in this paper on the basis of the mechanical properties of materials, at loads which are not in the neighbourhood of the ultimate load. The results obtained by means of this method are more or less generally applicable, and, at the same time, it is possible to estimate the effects of the separate factors. The amount of reinforcement, and the structural action of the concrete in tension after the formation of cracks, will be taken into account. To begin with, we shall study reinforced concrete prisms in tension as a basic type of structure.

Reinforced Concrete Prisms in Tension

Prior to the formation of cracks, the deformations can be calculated as usual, so as to take into account both the concrete and the reinforcement on the assumption that these two materials act together to the full extent in resisting the load. If the ratio of reinforcement is low, the effect of the reinforcement can, as a rule, be disregarded.

After the formation of cracks, the reinforcement will have to carry the whole load in a cross section through a crack. In the areas between the cracks the concrete will continue to carry part of the load. The total strain will be less than that which would be produced if the reinforcement bars were subjected throughout their length to the same stress as in the cracks.

For the following calculations, we introduce the notations given below.

- τ_{max} = the maximum bond stress.
 τ_{av} = the average value of the bond stress.
 σ_{ut} = the tensile strength of concrete (corresponding to the actual dimensions).
 $\sigma_{s-max}; \sigma_{s-av}$ = the maximum and the average stress in steel.

$\Delta \sigma_{s-max}$	= the maximum decrease of stress in steel.
$\Delta \sigma_{s-av}$	= the average value of the decrease of stress in steel.
ϵ	= the actual strain of the prism.
$\Delta \epsilon_{s-av}$	= the average value of the decrease in the strain of steel.
E_s	= the modulus of elasticity of steel.
d	= diameter of the reinforcement bars.
e	= the distance between the cracks.
A_c	= the cross-sectional area of the concrete.
A_s	= the cross-sectional area of the reinforcement.
A	= the cross-sectional area of the prism.
μ	= $\frac{A_s}{A} \sim \frac{A_s}{A_c}$.

Immediately before a crack is formed, the stress in this cross section of the concrete is equal to the tensile strength, and the total tensile force in the concrete is equal to the decrease in the tensile force in the reinforcement. The tensile stress in the concrete, just as in the reinforcement, can be assumed to be uniformly distributed over the cross section. Therefore, we obtain the following equation

$$\sigma_{ut} = \frac{A_s}{A_c} \Delta \sigma_{s-max} = \mu \Delta \sigma_{s-max} \quad (1)$$

In tension tests made on reinforced concrete prisms it has been found that the number of cracks increases with the strain up to a limit, see Fig. 1. As the strain increases, the force which can be transmitted from the reinforcement

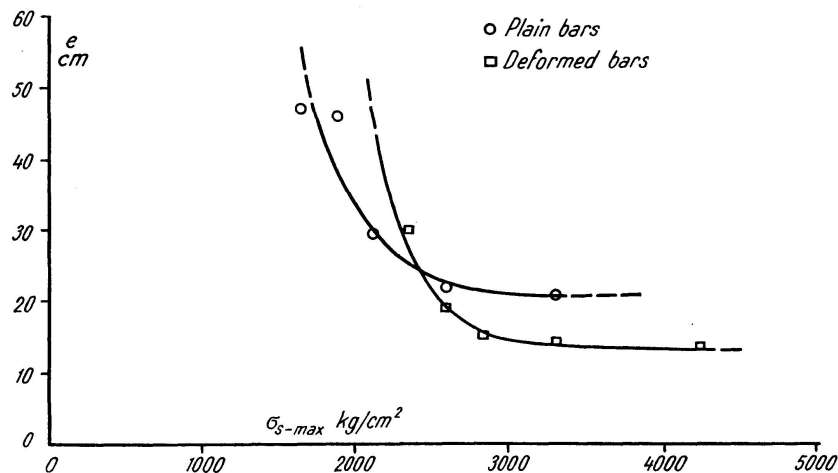


Fig. 1. Variation in the distance between cracks (e) with the stress in reinforcement determined from tension tests on reinforced concrete prisms

to the concrete through the bond between them becomes greater. Accordingly, the stress in the concrete increases, and the value of this stress in the middle between two cracks will be either less than, or equal to, the tensile strength. When corrected as shown below, Eq. (1) can be regarded as applicable to a

cross section between two cracks. Furthermore, it will be demonstrated that this statement can be considered to hold good also after the formation of cracks has come to an end.

Moreover, in order to be able to calculate the deformations, we must know the whole stress distribution between the cracks. This distribution is determined by the bond stress distribution. Many investigators have studied this subject, but their results are in many cases divergent. Therefore, we shall first make a general study of the effect produced by the distribution of bond on the deformations. In order to be able to calculate the total deformations, it is sufficient to know the mean value of the stress in steel. The maximum decrease in the stress in steel is obtained from the equation

$$\Delta \sigma_{s-max} = \frac{4}{d} \int_0^{\frac{e}{2}} \tau_x dx = \frac{2e}{d} \tau_{av} \quad (2)$$

By substituting

$$\Delta \sigma_{s-av} = k \Delta \sigma_{s-max} \quad (3)$$

we get from Eq. (1)

$$\Delta \sigma_{s-av} = \Delta \epsilon_{s-av} E_s = k \frac{\sigma_{ut}}{\mu} \quad (4)$$

Thus, so far as the bond stress is concerned, all that is required for the calculation of the deformations is to know its distribution between the cracks, i. e. the coefficient k . In this connection it is to be observed that Eq. (1) can be considered to hold good exactly for a given cross section only immediately before a crack is formed. In order to describe the state of stress in the middle between two cracks, Eq. (1) should be written

$$c \cdot \sigma_{ut} = \mu \cdot \Delta \sigma_{s-max}$$

where c is a constant which can theoretically be assumed to vary within the limits from 0,75 to 1 for the average of a great number of middle cross sections. Few tests are available for estimating the magnitude of the coefficient c , but these tests indicate that it is relatively close to unity. In what follows, we assume that the coefficient c is included in the coefficient k in Eq. (4). In other words, the coefficient k expresses a correction both for the effect on the distribution of bond on the deformations and for the approximation made in Eq. (1). In the fundamental discussion below, however we suppose that c is equal to unity. In the calculations, the distribution of bond is assumed to be symmetrical about $x = e/2$, see Fig. 2. If the distribution of bond is symmetrical about $x = e/4$ in the interval $0 \leq x \leq e/2$, but varies in a wholly arbitrary manner in all other respects, that is to say, if

$$\tau_x = \tau_{\frac{e}{2}-x}, \text{ we get } k = \frac{1}{2} \quad (5a)$$

This can be demonstrated by studying the curves representing $\Delta\sigma_s$, see Fig. 2. When τ is symmetrical about $x=e/4$, the curve $\Delta\sigma_s$ is twice reflected in $e/4$, with the result that the mean value becomes equal to half the maximum value. In addition to this type, there are also other distributions which can yield $k=\frac{1}{2}$, but they will be disregarded in this connection.

If τ_x is, for some value of x , greater than, but otherwise equal to, $\tau_{\frac{e}{2}-x}$, then a demonstration analogous to that given in the above proves that k is greater than $\frac{1}{2}$, that is to say,

$$\text{for } \tau_x \geq \tau_{\frac{e}{2}-x}, \text{ we get } k > \frac{1}{2} \tag{5b}$$

and similarly,

$$\text{for } \tau_x \leq \tau_{\frac{e}{2}-x}, \text{ we get } k < \frac{1}{2} \tag{5c}$$

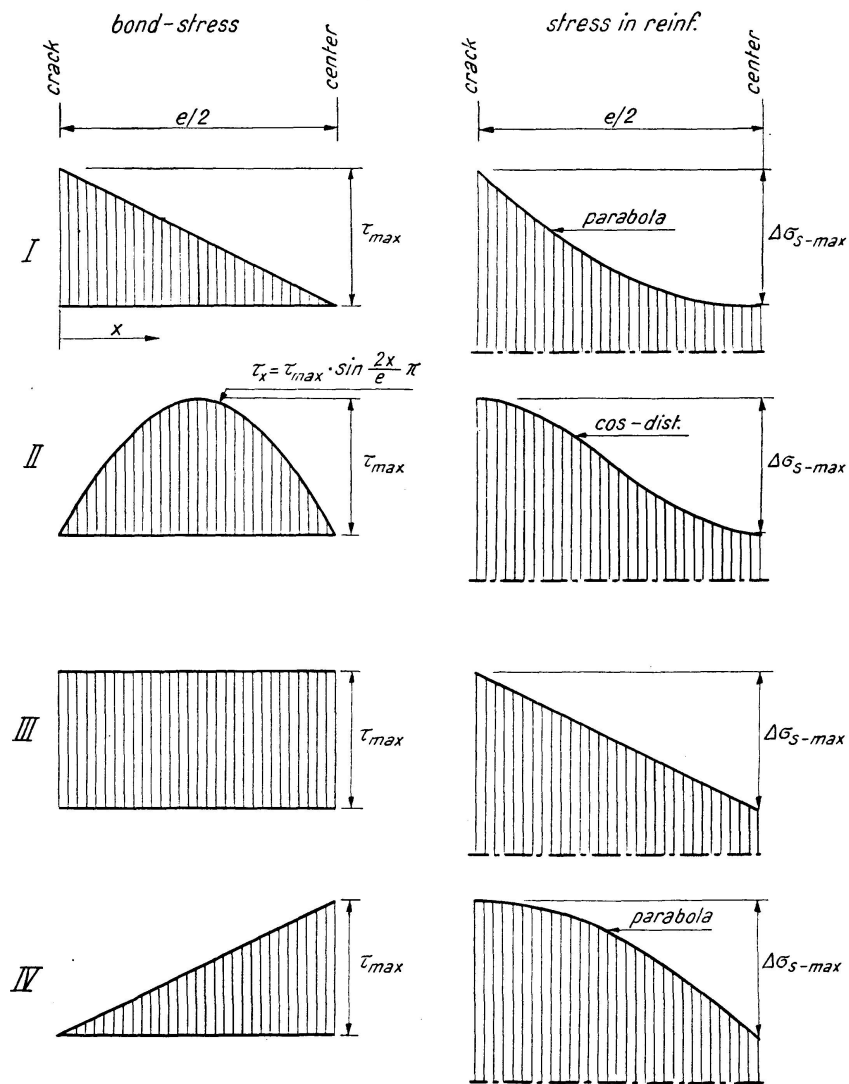


Fig. 2. Theoretical diagrams showing the distribution of bond stress and the corresponding distribution of stress in reinforcement

In order to obtain approximate limit values of k , we can study certain types of distribution of τ . These distributions will be termed „symmetrical“ if $k = \frac{1}{2}$, „positively skew“ if $k > \frac{1}{2}$, and „negatively skew“ if $k < \frac{1}{2}$. If it is required that the deformations should be small, then the distribution marked I in Fig. 2 is to be regarded as the most favourable. In concrete structures reinforced with deformed bars, this distribution can be obtained in an early stage of crack formation (the tests made by KUUSKOSKI¹⁾ show distributions which are approximately similar to this type), but it is soon superseded by distributions which are more closely in agreement with the types II or III. A distribution of the type I corresponds to $k = \frac{2}{3}$. Distributions of the types II and III are symmetrical, and both of them correspond to $k = \frac{1}{2}$ in accordance with the above. The type IV can, as a rule, be regarded as the most unfavourable distribution. It can be imagined to occur in a far-advanced stage of crack formation. This distribution corresponds to $k = \frac{1}{3}$. Consequently, we obtain the following limits for k :

$$\frac{2}{3} \gtrsim k \gtrsim \frac{1}{3}$$

It follows from tests that the value of $\Delta \epsilon_{s-av}$ shortly after the formation of cracks can be considered to be constant and independent of the magnitude of the strain, at any rate up to strains of about 3 pro mille, which has so far been the upper limit reached in the tests. Fig. 3 reproduces the results of

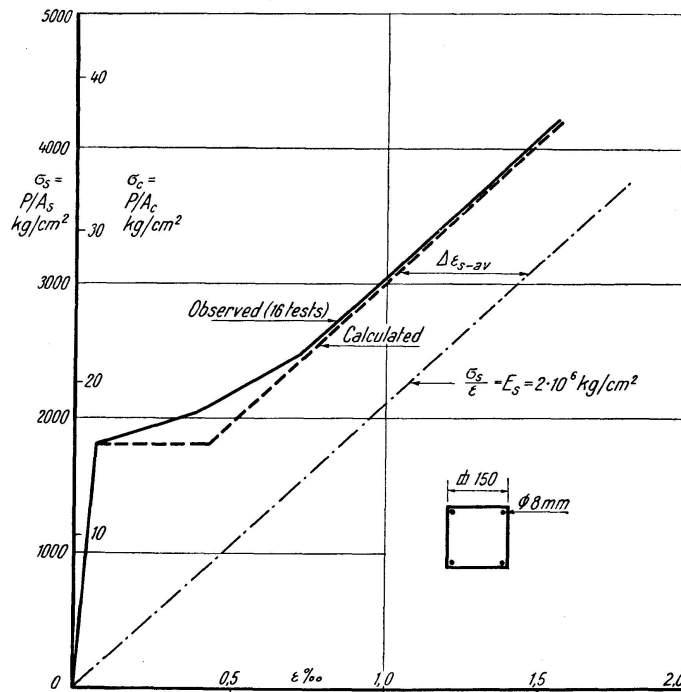


Fig. 3. Comparison of strains observed in tension tests on reinforced concrete prisms²⁾ and calculated from Eq. (6)

¹⁾ KUUSKOSKI, VILJO: Über die Haftung zwischen Beton und Stahl. Helsinki 1950.

tests made at the Institution of Building Statics and Structural Engineering of the Royal Institute of Technology, Stockholm²). The test specimens were provided with two types of reinforcement, viz., plain bars and deformed bars. The deformations observed in the tests were found to be equal, irrespective of the type of reinforcement. The test specimens were partly moist-cured, and partly dry-cured. The rate of increase in load was $\approx 200 \text{ kg/cm}^2$ per min. The gauge length was 50 cm. Ratio of reinforcement = 0.89%. The mean value obtained from 16 tests was $\Delta \epsilon_{s-av} = 0,52 \frac{\sigma_{ut}}{\mu E_s}$, i. e.

$k = 0,52$. The formation of cracks in these tests is represented in Fig. 1. A comparison shows that $\Delta \epsilon_{s-av}$ remains constant also after the formation of cracks has come to an end. Therefore, we can assume that Eq. (1), with the approximations made in the above, is also applicable under these conditions. The bond stress distribution may be taken to be in relatively close agreement with one of the "symmetrical" types shown in Fig. 3. In a relatively early stage of strain in tests made on concrete specimens reinforced with deformed bars, the tests made by KUUSKOSKI show "positively skew" distributions, which nearly resembled the type I in Fig. 3, whereas the distributions in the case of plain bars were slightly "positively skew", and were closely similar to the symmetrical distribution of the type III. The tests made by BRICE and BICHARA³) show "positively skew" distributions in the case of deformed bars at small strains, while the distributions at greater strains were slightly "negatively skew". However, none of the above-mentioned investigators has made any measurements in order to determine the distribution of bond after the formation of a great number of cracks. The value of k computed from the results of KUUSKOSKI's tests is slightly greater than 0,5 (if the influence of the coefficient c is taken into account), whereas the corresponding value obtained from BRICE's and BICHARA's results is slightly less than 0,5. The fact that the latter value is lower can be due to the method of load application. This will be mentioned further on. To sum up the tests reviewed in the above, we find that $\Delta \epsilon_{s-av}$ after the formation of cracks can be regarded as constant, and that it can to a close approximation be calculated from Eq. (4) if we put $k = 0,5$.

The average decrease of the stress in steel, $\Delta \sigma_{s-av}$, has been calculated by means of Eq. (4) for several values of σ_{ut} and μ . The results are reproduced in Table 1. Since the difference between the maximum and minimum values of the stress in reinforcement is twice as great, it follows that the measurements of the strain of reinforcement over a small gauge length will be strongly affected by the position of the gauge with respect to the crack configuration.

²) NYLANDER, HENRIK: Korsarmerade betongplattor (Concrete Slabs Reinforced in Two Directions), Betong 35 (1950).

³) BRICE, L. P.: Adh rence des barres d'acier dans le b ton. Annales de l'institut Technique du B timent et des Travaux Publics, Mars-Avril 1951, No. 19.

Table 1. Average decrease in the stress in reinforcement, in kg per cm², due to the contributive effect of concrete in prismatic tension test specimens, $k=0,5$ (see Eq. (4))

$\mu \backslash \sigma_{ut}$	10 kg/cm ²	20 kg/cm ²	30 kg/cm ²
0,004	1250	2500	3750
0,006	830	1700	2500
0,008	620	1250	1900
0,010	500	1000	1500
0,015	330	670	1000
0,020	250	500	750
0,030	170	330	500

A separate measurement of this kind affords information only on the stress at the gauge point, but does not give any accurate idea of the total force or the mean strain. An analogous conclusion can also be drawn regarding the measurement of the strain of the tensile reinforcement in concrete beams, as will be shown in the next section.

It follows from the above that the total strain of a reinforced concrete prism after the formation of cracks can be considered to be dependent only on the tensile strength of the concrete and the amount of reinforcement, whereas it is independent of the diameter of the reinforcement bars, the modulus of elasticity of the concrete, and the bond strength. The total strain ($k=0.5$) can be calculated from the equation

$$\epsilon = \frac{1}{E_s} \left(\frac{P}{A_s} - k \frac{\sigma_{ut}}{\mu} \right) \approx \frac{1}{E_s} \left(\sigma_{s-max} - 0,5 \frac{\sigma_{ut}}{\mu} \right) \quad (6)$$

whence

$$\sigma_{s-av} = \sigma_{s-max} - k \frac{\sigma_{ut}}{\mu} \approx \sigma_{s-max} - 0,5 \frac{\sigma_{ut}}{\mu} \quad (7)$$

The above equations hold good on the assumption that the reinforcement bars are not exposed to creep. If the load is applied at a slow rate, or if it is maintained constant at a certain definite value, the reinforcement bars will slowly creep in the concrete, and the structural action of the concrete will be weakened. A similar effect is produced by alternate loading. As a result, the bond between steel and concrete breaks down, $\Delta \epsilon_{s-av}$ decreases, and the strain approaches the value corresponding to a reinforcement bar which is not embedded in concrete, see above. This value is the upper limit of the deformations; the lower limit is obtained from Eq. (6). If the reinforcement consists of plain bars, the reduction in the structural action of the concrete is greater than in the case of deformed bars. Furthermore, it is necessary to take into account the fact that the strength of concrete subjected to long-time loads is smaller than that obtained under short-time loads. The influence of shrinkage can be disregarded in the calculation of the total deformation, as will be shown below.

Reinforced Concrete Beams Submitted to Moments

Prior to the formation of cracks, the stiffness, and hence also the deformations, can be calculated by means of the usual method taking into account both the concrete and the reinforcement on the assumption that these two materials act together to the full extent in resisting the load. As a rule, the effect of the reinforcement can be disregarded.

Assumptions and Definitions

After the formation of cracks, the tensile reinforcement must be taken into account. In the cracked portion of the beam on the side in tension, the concrete is effective only between the cracks. As a rule, the concrete in tension between the interior part of a crack and the neutral axis can be disregarded, whereas the concrete in tension between the cracks cannot be neglected.

In order to calculate the deformations, we assume that two cross sections which are in the same position with respect to the crack configuration, or which are so far apart that any difference in their respective positions can be disregarded, remain plane in relation to each other. Measurements made by many investigators show that this assumption is at least approximately correct.

The stress distribution between the reinforcement and the concrete in tension is assumed to be analogous to that in reinforced concrete prisms. Accordingly, the stress at the bottom of the beam reaches the tensile strength in bending of the concrete immediately before the formation of a crack.

The stress-strain curve of the concrete is supposed to be rectilinear both in compression and in tension. Normally, it is of interest to determine the deformations at those compressive stresses which are not in the neighbourhood of the ultimate strength. The above assumption is therefore in this case to be considered as a relatively close approximation. On the side in tension, the concrete in a cross section in the middle between two cracks will be submitted to a stress which is equal to its ultimate strength. In this case, too, the assumed rectilinear stress distribution is to be considered as a relatively close approximation since the maximum stress is set up in the middle section only. Furthermore, it is to be expected that a triangular stress distribution on the side in tension will agree with the actual conditions as closely as, for instance, a rectangular stress distribution, even shortly before failure. Even a relatively large deviation from the above-mentioned assumptions regarding a rectilinear stress-strain curve have but a slight influence on the final results obtained in what follows.

We introduce the following notations:

M = the moment acting on the beam.

$\sigma_{sII}, \epsilon_{sII}$ = the stress in steel and the strain of steel calculated on the assumptions corresponding to the stage II.

- $\sigma_{cII}, \epsilon_{cII}$ = the stress in concrete in compression and the strain of concrete in compression calculated on the assumptions corresponding to the stage II.
- $\left. \begin{array}{l} \Delta \sigma_{s-max}, \Delta \sigma_{s-av} \\ \Delta \epsilon_{s-max}, \Delta \epsilon_{s-av} \end{array} \right\}$ = the maximum decrease and the average decrease of the stress in steel and the strain of steel due to the action of the concrete in tension.
- $\left. \begin{array}{l} \Delta \sigma_{c-max}, \Delta \sigma_{c-av} \\ \Delta \epsilon_{c-max}, \Delta \epsilon_{c-av} \end{array} \right\}$ = the maximum decrease and the average decrease of the stress in concrete in compression and the strain of concrete in compression due to the action of the concrete in tension.
- σ_{uf} = the tensile strength in flexure of the concrete (corresponding to the actual dimensions).
- σ_{cf-av} = the average tensile stress in the concrete in flexure.
- E_c = the modulus of elasticity of the concrete (effect of plastic flow taken into account too).
- EJ = the flexural rigidity.
- E_{id} = the idealised modulus of elasticity $\left(= \frac{12(EJ)}{bH^3}$ for a rectangular cross section).
- ρ_s = the internal lever arm of the reinforcement.
- M_f = $\frac{bH^2\sigma_{uf}}{6}$ = the moment causing the formation of cracks.
- H = the total depth of the beam.
- h = the distance from the centre of the reinforcement to the top surface of the beam.
- b = the width of the beam.
- $c \cdot h$ = the depth of the compressive concrete zone
- $c_{II} \cdot h$ = the depth of the compressive concrete zone calculated on the assumptions corresponding to the stage II.
- n = $\frac{E_s}{E_c}$
- μ = $\frac{A_s}{bh}$

In the stage II, the concrete in tension is completely disregarded, and the stress-strain curve of the concrete in compression is assumed to be rectilinear. In other words, the calculation is in accordance with the classical method. This calculation yields

$$\sigma_{sII} = \frac{M}{\mu b h^2 \left(1 - \frac{c_{II}}{3}\right)}; \quad \epsilon_{sII} = \frac{\sigma_{sII}}{E_s} \quad (8a \text{ and } 8b)$$

$$\sigma_{cII} = \frac{2M}{b h^2 c_{II} \left(1 - \frac{c_{II}}{3}\right)}; \quad \epsilon_{cII} = \frac{\sigma_{cII}}{E_c} \quad (9a \text{ and } 9b)$$

$$c_{II} = n\mu \left(\sqrt{1 + \frac{2}{n\mu}} - 1 \right) \quad (10)$$

Owing to the effect of the concrete in tension, the actual deformations are smaller than those calculated on the assumptions corresponding to the stage II. The resultant reduction in the deformations can be determined by computing the moment acting on the concrete in tension and the corresponding concrete in compression in each cross section. The assumed stress distribution in a given cross section between the cracks is shown in Fig. 4. The tensile stress in bending varies from a certain definite value at the edge to zero at the neutral axis. The compressive stress varies in a corresponding manner. This implies that an individual cross section does not remain plane after the formation of cracks, since the tensile stress can be considered to be constant, or at

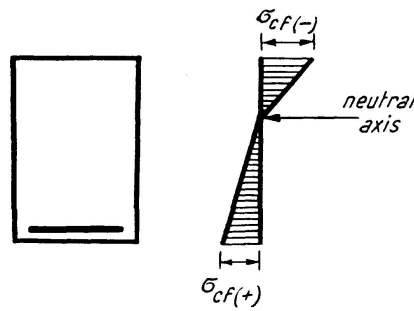


Fig. 4. Assumed stress distribution in concrete between the cracks

least to be lower than a certain definite value, whereas the compressive stress increases as the load becomes greater. The neutral axis will be transformed into a wave-shaped line along the beam, so that the wave crests are in the neighbourhood of the cracks, while the wave troughs are between the cracks. The calculations are based on the middle position of the neutral axis along the beam. This is a negligible approximation. The stress in reinforcement and the tensile stress in bending are assumed to be dependent on the τ -distribution in their respective manners, and the variation in this distribution is supposed to be analogous to that in reinforced concrete prisms, cf. Fig. 2. In order to calculate the deformations, it is sufficient to know the mean values of $\Delta\sigma_s$ and $\Delta\sigma_{cf}$. By analogy with Eq. (3), we put

$$\frac{\Delta\sigma_{s-av}}{\Delta\sigma_{s-max}} = \frac{\Delta\sigma_{cf-av}}{\Delta\sigma_{cf}} = k \quad (11)$$

Just as in the case of reinforced concrete prisms, we suppose that the coefficient k takes into account the influence of the τ -distribution and the approximation due to the assumption that the concrete in a cross section in the middle between two cracks is submitted to a stress which is equal to its tensile strength in bending.

The average moment to be resisted by the concrete in tension along the beam is

$$\Delta M_{c-av} = \frac{k \cdot \sigma_{uf} \cdot b H (H - ch)}{3} = 2 k M_f \left(1 - c \frac{h}{H}\right) \quad (12)$$

Deformations of Beams on the Side in Tension

The moment expressed by Eq. (12) corresponds to the average reduction in the load to be resisted by the tensile reinforcement. Hence we can calculate $\Delta \sigma_{s-av}$

$$\Delta \sigma_{s-av} A_s \rho_s = \Delta \sigma_{s-av} A_s h \left(1 - \frac{c}{3}\right) = \Delta M_{c-av} \quad (13)$$

If the values of ΔM_{c-av} and ρ_s calculated on the assumptions corresponding to the stage II are inserted in Eq. (13), we obtain the asymptotic value which $\Delta \sigma_{s-av}$ approaches as the load increases. In an earlier stage, we have, as a rule, $c > c_{II}$. In that case, as can be seen from Eqs. (12) and (13), both ΔM_{c-av} and ρ_s are less than their respective asymptotic values. The decrease in ΔM_{c-av}

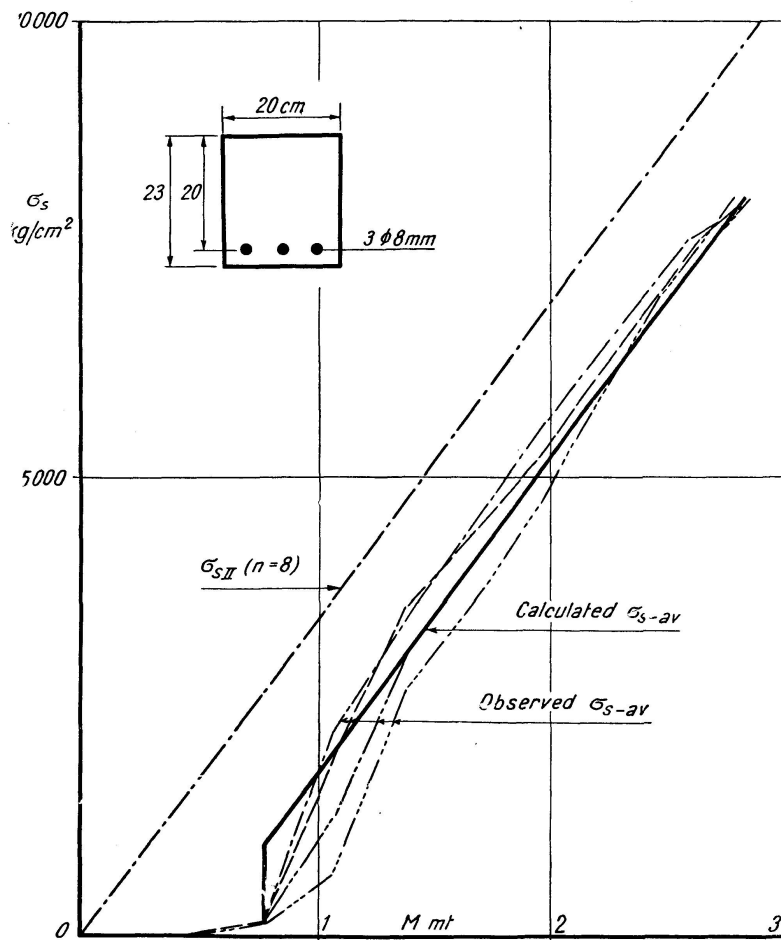


Fig. 5. Comparison of stresses in reinforcement observed in tests³⁾ and calculated from Eq. (17a)

is somewhat greater than that in ρ_s , but this is outbalanced by the resistance of the concrete in tension between the internal parts of the cracks and the neutral axis, which has been disregarded in the deduction of Eq. (12) in accordance with the above assumptions. Since the ratio of ΔM_{c-av} to ρ_s determines the magnitude of $\Delta \sigma_{s-av}$, we can put $\Delta \sigma_{s-av}$ approximately equal to the asymptotic value, that is to say, we can assume that $\Delta \sigma_{s-av}$ is constant and independent of the magnitude of the load after the formation of cracks. This assumption is in accordance with the results obtained in the study of reinforced concrete prisms. Furthermore, this assumption is also in agreement with test results, see Fig. 5⁴).

By inserting $c = c_{II}$ in Eq. (13), we obtain

$$\Delta \sigma_{s-av} = \frac{k \sigma_{uf} \left(1 - \frac{h}{H} c_{II}\right)}{3 \mu \left(1 - \frac{c_{II}}{3}\right)} \left(\frac{H}{h}\right)^2 = \frac{2 k M_f \left(1 - \frac{h}{H} c_{II}\right)}{b h^2 \mu \left(1 - \frac{c_{II}}{3}\right)} \quad (14)$$

If we assume an approximate "symmetrical" distribution of bond, i. e. if $k = 0,5$ and choose $h = 0,92 H$, we get

$$\Delta \sigma_{s-av} = 0,20 \frac{\sigma_{uf}}{\mu} \frac{1 - 0,92 c_{II}}{1 - \frac{c_{II}}{3}} \quad (15)$$

It is seen from Eq. (15) that the decrease $\Delta \sigma_s$ is dependent not only on μ , but also on c_{II} , and hence on n in conformity with Eq. (10). In the interval $0,015 < n \mu < 0,15$, which comprises most beams submitted to short-time loads ($E_c \gtrsim 180,000 \text{ kg/cm}^2$), the variation due to $n \mu$ can be neglected, and Eq. (15) can be written

$$\Delta \sigma_{s-av} \approx 0,16 \frac{\sigma_{uf}}{\mu}; \quad (0,015 \lesssim n \mu \lesssim 0,15) \quad (16)$$

Thus we get

$$\sigma_{s-av} = \sigma_{sII} - 0,16 \frac{\sigma_{uf}}{\mu}; \quad \epsilon_{s-av} = \frac{\sigma_{s-av}}{E_s} \quad (17a \text{ and } 17b)$$

The quantity σ_{sII} is obtained from Eq. (8a).

The value of $\Delta \sigma_{s-av}$ calculated from Eq. (16) for the smaller value of $n \mu$ is about 10 per cent lower than that computed from Eq. (15), whereas the corresponding value obtained for the greater value of $n \mu$ is about 10 per cent higher. As a rule, considering the difficulties of estimating σ_{uf} , this approximation can be regarded as satisfactory.

For higher values of $n \mu$, which are usually obtained in the case of long-time loading ($E_c \lesssim 120,000 \text{ kg/cm}^2$, this is the effective modulus of elasticity taken into account the effect of plastic flow), the variation in $n \mu$ cannot be disregarded. In that case, Eq. (15) can be written

⁴) ABELES, P.: Versuche mit Rechteckbalken, bewehrt mit besonders hochwertigem Stahl. Beton und Eisen, 1939.

$$\Delta \sigma_{s-av} \approx 0,08 \frac{\sigma_{uf}}{\mu^4 \sqrt{n\mu}}; \quad (0,15 \lesssim n\mu \lesssim 6) \quad (18)$$

Hence we get

$$\sigma_{s-av} = \sigma_s - 0,08 \frac{\sigma_{uf}}{\mu^4 \sqrt{n\mu}}; \quad \epsilon_{s-av} = \frac{\sigma_{s-av}}{E_s} \quad (19a \text{ and } 19b)$$

The quantity σ_{sII} is obtained from Eq. (8a).

Eq. (18) involves an error which is less than about 4 per cent in relation to Eq. (15).

The values of $\Delta \sigma_{s-av}$ computed by means of Eq. (16) are given in Table 2.

The values of $\Delta \sigma_{s-av}$ calculated by the aid of the above method have been checked by comparing them with the average strains observed in tests on four similar beams, see Fig. 5. These tests had been made by ABELES⁴). Considering the difficulty of determining σ_{uf} from the available data and the influence of shrinkage in the course of curing, the agreement is to be regarded as good.

Table 2. Average decrease in the stress in reinforcement, in kg per cm², due to the contributive effect of concrete in tension in concrete beams (see Eq. 16))

$\mu \backslash \sigma_{uf}$	10 kg/cm ²	20 kg/cm ²	40 kg/cm ²	60 kg/cm ²
0,002	800	1600	3200	4800
0,004	400	800	1600	2400
0,006	270	530	1100	1600
0,008	200	400	800	1200
0,010	160	320	640	960
0,015	110	210	430	640
0,020	80	160	320	480
0,030	50	100	210	320

Deformations of Beams on the Side in Compression

In the calculation of $\Delta \sigma_c$, the variation due to $n\mu$ cannot be neglected. An exact calculation based on the previous assumptions would be very laborious, and is not justified by the accuracy in the assumptions. In the calculation of the flexural rigidity by means of Eq. (22), see below, $\Delta \epsilon_c$ is small in comparison with the other factors. Even a rough approximation of $\Delta \epsilon_c$ is therefore sufficient for the calculation of the flexural rigidity. The stress in concrete at the top of the beam can be written ($k=0.5$)

$$\sigma_{c-av} = \sigma_{cII} - \Delta \sigma_c = \sigma_{cII} \left(1 - \frac{0,12}{3\sqrt{n\mu}} \frac{M_f}{M} \right); \quad \epsilon_{c-av} = \frac{\sigma_{c-av}}{E_c} \quad (20a \text{ and } 20b)$$

The quantity σ_{cII} is obtained from Eq. (9a).

It is to be observed that these equations yield only a relatively rough approximation to the value of $\Delta \sigma_c$. This approximation is sufficient for calculating the deformations of the whole cross section, but a relatively large percentage deviation can be obtained in comparison with test results expressing the value of $\Delta \sigma_c$ alone. If an accurate value of $\Delta \sigma_c$ is required, the solution must be rendered more exact, but in that case it will be relatively intricate.

Position of Neutral Axis

The distance x from the neutral axis to the top surface of the beam can be expressed by

$$x = h \frac{\epsilon_{cII} - \Delta \epsilon_c}{\epsilon_{cII} - \Delta \epsilon_c + \epsilon_{sII} - \Delta \epsilon_s} \quad (21a)$$

If the beams are provided with a relatively small amount of reinforcement, $\Delta \epsilon_c$ can be disregarded, and Eq. (21a) can be written

$$x \approx h \frac{\epsilon_{cII}}{\epsilon_{cII} + \epsilon_{sII} - \Delta \epsilon_s} \quad (21b)$$

As the stress becomes greater, the effect of $\Delta \epsilon_s$ decreases, and the numerator increases in relation to the denominator, with the result that x decreases. In other words, since the contributive effect of the concrete in tension is reduced as the load increases, the neutral axis passes to a higher level and asymptotically approaches its limiting position in beams provided with a relatively small amount of reinforcement.

If the beams are provided with a very large amount of reinforcement, the influence of the contributive effect of the concrete in tension on the deformations is slight. On the other hand, the compressive stress in the concrete becomes high as the load increases. The modulus of elasticity of the concrete will therefore decrease, with the result that the neutral axis will sink to a somewhat lower level.

Flexural Rigidity and Idealised Modulus of Elasticity

The flexural rigidity can now be calculated by using the expressions for $\Delta \sigma_{s-av}$ and $\Delta \epsilon_{s-av}$ given by Eq. (14) and the expression for ϵ_{c-av} given by Eq. (20b). After simplification, we obtain

$$\frac{1}{EJ} = \frac{\epsilon_{s-av} + \epsilon_{c-av}}{hM} = \frac{2n\mu + c_{II}}{bh^3 c_{II} \left(1 - \frac{c_{II}}{3}\right) \mu E_s} \cdot \left[1 - \frac{2 \left[0,12^{2/3} \sqrt{n\mu} + k \left(1 - \frac{h}{H} c_{II}\right) c_{II} \right] \frac{M_f}{M}}{2n\mu + c_{II}} \right] = \beta \frac{1}{bh^3 \mu E_s} \cdot \left[1 - \gamma \frac{M_f}{M} \right] \quad (22)$$

In order to deduce an expression that is suited for practical use, it is necessary to simplify β and γ . Just as in the above, it proves difficult to find an approximation which holds good for all values of $n\mu$, and which is accurate and simple at the same time. This approximation is therefore carried out in two intervals. The approximation made in this case results in an error of less than about 5 per cent in Eq. (23a) and an error of less than about 10 per cent in Eq. (23b), see below. The agreement in the derivative is not so good. If we put $h=0.92 H$ and $k=0.5$, we obtain the following two equations for the idealised modulus of elasticity:

$$E_{id} = \frac{\mu E_s}{0,28 \sqrt[6]{n\mu} - \frac{0,065 M_f}{\sqrt[6]{n\mu} M}}; \quad (0,015 \lesssim n\mu \lesssim 0,15) \quad (23 a)$$

$$E_{id} = \frac{\mu E_s}{0,53 \sqrt[6]{n\mu} - 0,10 \frac{M_f}{M}}; \quad (0,15 \lesssim n\mu \lesssim 2) \quad (23 b)$$

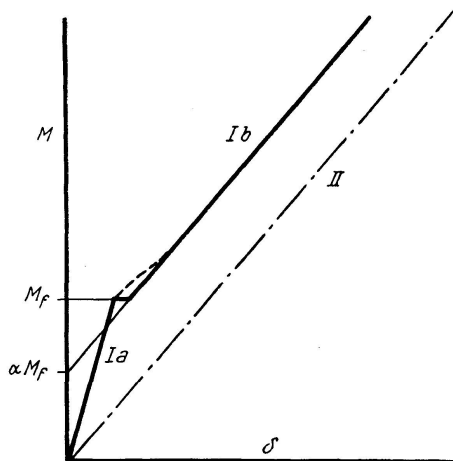


Fig. 6. Theoretical shape of deflection curve. The short-dash line curves indicate the approximate actual shape of the upper limit curve

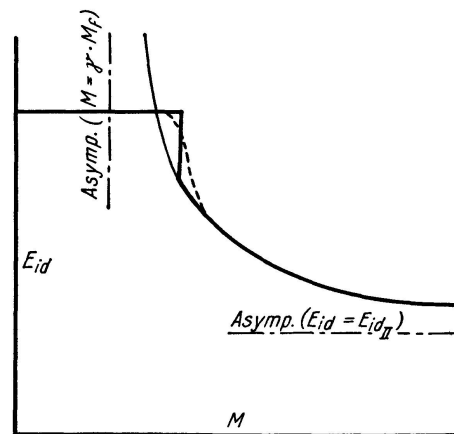


Fig. 7. Theoretical shape of the idealised modulus of elasticity curve corresponding to the deflection curve shown in Fig. 6

A typical shape of the moment-deflection curve is shown in Fig. 6. The deflection curve before the development of cracks (marked *Ia* in Fig. 6) starts from the origin, and its slope is determined by EJ calculated for the whole cross section. After the development of cracks, the deflection curve (marked *Ib* in Fig. 6) starts from a point having the ordinate = γM_f , where γ is determined by Eq. (22) and the following equations. The slope of this line is determined by Eq. (23) for $M_f=0$, and corresponds to the slope calculated on the assumptions characterising the stage II (see the line marked *II* in Fig. 6). Consequently, the deformation after the development of cracks will be equal

to that calculated on the assumptions corresponding to the stage II, δ_{II} , with the deduction of a constant value $\Delta\delta$, that is to say,

$$\delta = \delta_{II} - \Delta\delta \quad (24)$$

The idealised modulus of elasticity corresponding to the deflection curve I is represented in Fig. 7. It is constant until the formation of cracks, and then passes into a hyperbolic curve which is determined by Eq. (23). The asymptote which is approached by the hyperbola as the load increases is given by E_{id} calculated on the assumptions characterising the stage II. The position of the other asymptote of the hyperbola is determined by the intersection of the line Ib and the axis of ordinates (the point γM_f). As has already been pointed out, the simplified assumptions made in the above do not hold good in the neighbourhood of failure. In that case, the deformations increase at a considerably higher rate, and are, as a rule, greater, than those computed on the assumptions corresponding to the stage II. The idealised modulus of elasticity E_{id} is shown in Fig. 8 for several values of E_c , M_f , and μ . As has been mentioned in the above, most beams submitted to short-time loads ($E_c \gtrsim 180,000$ kg/cm²) fall under the interval $0.015 \lesssim n\mu \lesssim 0.15$, while most beams subjected to long-time loads ($E_c \lesssim 120,000$ kg/cm²) come within the interval $0.15 \lesssim n\mu \lesssim 2$.

Just as in the case of reinforced concrete prisms in tension, it is to be noted that alternate loads and long-time loads impair the bond between the concrete and the reinforcement. The contributive effect of the concrete in tension decreases, $\Delta\delta$ (or γM_f) becomes smaller, and the deformations approach the values computed on the assumptions characterising the stage II. At the same time, ϵ_{s-ar} and ϵ_{c-ar} undergo corresponding changes. Inadequate anchorage can constitute another disturbing factor. If sliding takes place on account of an excessively high bond stress, then ϵ_s will increase. The effect of this increase is equivalent to that of a decrease in E_s .

Since the contributive effect of the concrete in tension is dependent on the method of loading, the actual shape of the deflection curve is usually difficult to determine in an accurate manner. On the other hand, it is possible to calculate two limit curves for the deflections, viz., the upper limit curve corresponding to the full contributive effect of the concrete in tension, and the lower limit curve corresponding to the complete cessation of this contributive effect. These curves are marked I and II respectively in Fig. 6. The corresponding upper limit curves for the idealised moduli of elasticity are the hyperbolas in Fig. 8 calculated by means of Eq. (23), whereas the lower limit curves are represented by the horizontal asymptotes. Under unfavourable conditions, if the reinforcement is exposed to sliding on account of inadequate anchorage, and in the neighbourhood of failure, the deflections can exceed the values calculated on the assumptions corresponding to the stage II.

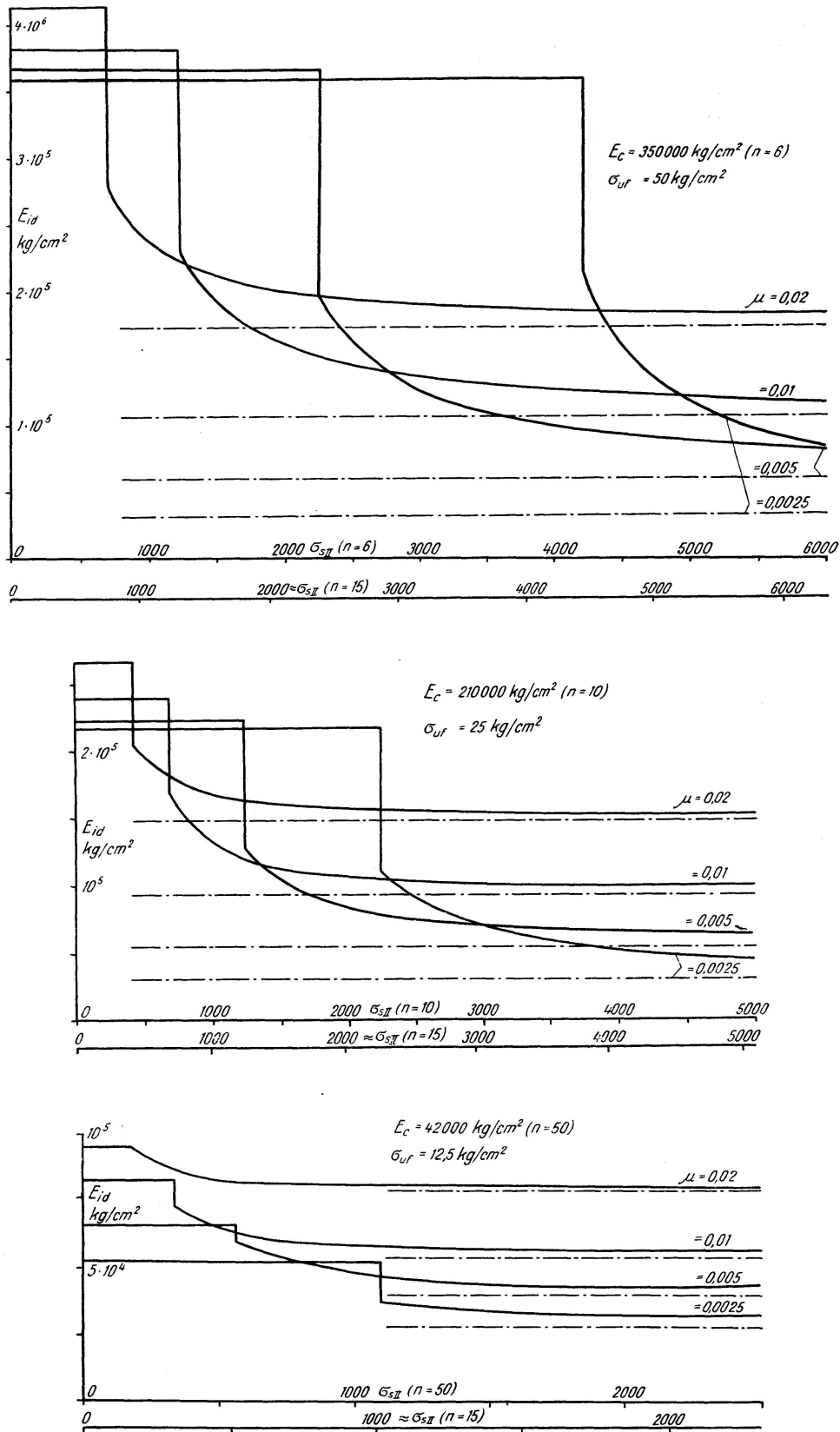


Fig. 8. Calculated limit curves for the idealised modulus of elasticity. The full-line curves represent the upper limit, whereas the dash-and-dot line horizontal asymptotes correspond to the lower limit (σ_s in kg/cm^2)

In the above we have dealt with beams of rectangular cross section. The equations for *T beams* can be deduced in an analogous manner. It is often sufficient to use the following approximate method of calculation, in which the equations given in the above can be employed directly. If the flange (width = B) of a T beam is subjected to compression, this beam is treated as a beam of rectangular cross section whose width is equal to the width of the rib (width = b). A value of the modulus of elasticity of the concrete which is equal to B/b times its actual value is then inserted in the formulæ deduced in the above. If the flange of the T beam is submitted to tension, this beam is regarded as a beam of rectangular cross section whose width is equal to the width = B of the flange, and the value of the modulus of elasticity of the concrete to be inserted in the formulæ is put equal to b/B times its actual value.

The above formulæ can also be used for designing beams with *compression reinforcement* if the modulus of elasticity of the concrete is corrected so as to allow for the compression reinforcement.

Furthermore, the results obtained in the above can be applied to *prestressed beams* if M_f and the amount of reinforcement are corrected so as to allow for the magnitude of the initial stress. Moreover, these results are applicable in a corresponding manner to beams subjected to combined compression and bending.

In dealing with those beams which primarily fail on the side in compression, the contributive effect of the concrete in tension is of importance in determining the ultimate compression of the concrete.

Distance between Cracks and Widths of Cracks

Notations:

- e = the distance between cracks.
- δ = the width of cracks.
- ϵ_{sh} = the shrinkage of the concrete.

For *reinforced concrete prisms* in tension, we obtain from Eqs. (1) and (2), for all types of τ -distributions, the distance between cracks

$$e = \frac{d \sigma_{ut}}{2 \tau_{av} \mu} \quad (25)$$

The basic equation for calculating the width of cracks is

$$\delta = e (\epsilon_s - \Delta \epsilon_{s-av} - \epsilon_c + \epsilon_{sh}) \quad (26)$$

By inserting the values of e and $\Delta \epsilon_{s-av}$ obtained in the above and $k=0.5$, we get

$$\delta = \frac{d \sigma_{ut}}{2 \tau_{av} \mu} \left(\epsilon_s - \frac{0,5 \sigma_{ut}}{\mu E_s} - \frac{0,5 \sigma_{ut}}{E_c} + \epsilon_{sh} \right) \quad (27)$$

where

$$\epsilon_s = \frac{P}{A_s E_s}$$

For reinforced concrete beams, the width of cracks is calculated in the same manner as in the case of concrete prisms, and we obtain, for all types of τ -distributions, the expressions

$$e = \frac{0,16 d \sigma_{uf}}{\tau_{av} \mu}; \quad (0,015 \lesssim n \mu \lesssim 0,15) \quad (28a)$$

$$e = \frac{0,08 d \sigma_{uf}}{\tau_{av} \mu^4 \sqrt{n \mu}}; \quad (0,15 \lesssim n \mu \lesssim 6) \quad (28b)$$

The basic equation for calculating the width of cracks on a level with the reinforcement is

$$\delta = e (\epsilon_{sII} - \Delta \epsilon_{s-av} - \epsilon_c + \epsilon_{sh}) \quad (29)$$

The values of e and $\Delta \epsilon_{s-av}$ obtained in the above and $k=0.5$ are inserted in this equation. Furthermore, we substitute for ϵ_c that value which holds good for the bottom surface of the beam. The resulting value of ϵ_c on a level with the reinforcement is therefore slightly too high, but this difference is negligible. We obtain

$$\delta = \frac{0,16 d \sigma_{uf}}{\tau_{av} \mu} \left(\epsilon_{sII} - \frac{0,16 \sigma_{uf}}{\mu E_s} - \frac{0,5 \sigma_{uf}}{E_c} + \epsilon_{sh} \right); \quad (0,015 \lesssim n \mu \lesssim 0,15) \quad (30a)$$

$$\delta = \frac{0,08 \sigma_{uf}}{\tau_{av} \mu^4 \sqrt{n \mu}} \left(\epsilon_{sII} - \frac{0,08 \sigma_{uf}}{\mu^4 \sqrt{n \mu} E_s} - \frac{0,5 \sigma_{uf}}{E_c} + \epsilon_{sh} \right); \quad (0,15 \lesssim n \mu \lesssim 6) \quad (30b)$$

Eq. (30a) can also be used for $n \mu \gtrsim 0.15$, but the values of δ obtained in that case will be too high.

In the above equations for determining the widths of cracks in reinforced concrete prisms and beams, the second and the third terms in brackets represent the effect of the concrete in tension. Alternate loads and long-time loads reduce this effect. If the contributive effect of the concrete in tension completely vanishes, then both these terms become equal to zero, and we obtain the greatest width of cracks. However, even under unfavourable conditions, the concrete in tension will usually produce some contributive effect. If this favourable contributive effect is put approximately equal to the unfavourable influence of shrinkage, we obtain the following maximum values of the width of cracks, which hold good for all distributions of bond:

$$\text{Prisms:} \quad \delta_{max} \lesssim \frac{d \sigma_{ut}}{2 \tau_{av} \mu} \epsilon_s \quad (31)$$

$$\text{Beams: } \delta_{max} \lesssim \frac{0,16 d \sigma_{uf}}{\tau_{av} \mu} \epsilon_{sII}; \quad (0,015 \lesssim n \mu \lesssim 0,15) \quad (32a)$$

$$\delta_{max} \lesssim \frac{0,08 d \sigma_{uf}}{\tau_{av} \mu^4 \sqrt{n \mu}} \epsilon_{sII}; \quad (0,15 \lesssim n \mu \lesssim 6) \quad (32b)$$

These values constitute the upper limit values for the magnitude of the widths of cracks, whereas those given above are the lower limit values. Eq. (32a) can also be used for $n \mu > 0.15$, but the values obtained in that case are on the safe side.

It is to be observed that the widths of cracks calculated in the above are mean values. The actual widths of cracks will exhibit a certain dispersion around these values on account of the dispersion in the influencing factors. For instance, the maximum width of cracks in a long beam will therefore usually be greater than that in a short beam, other conditions being equal.

That factor in the above formulæ which is, as a rule, most difficult to determine is τ_{av} . For example, the bond strength varies with the character of the surface of the reinforcement bars and with the properties of the concrete, and probably also with the diameter of the reinforcement bars. A detailed study of the influence of these factors on the bond strength lies beyond the scope of the present paper. Such a study requires special investigations^{1) 3) 5)}.

Reinforced Concrete Slabs

The deformations of a reinforced concrete slab prior to the development of cracks can be calculated in the same manner as the deformations of an isotropic slab having the thickness = H and the modulus of elasticity = E_c . It is usually sufficient to assume that POISSON'S ratio = ν is equal to zero.

After the formation of cracks, the problem becomes more complicated. If the amounts of reinforcement are not the same in different directions, then the slab is anisotropic. The most difficult problem is to determine the torsional rigidity of the slab. Diagonal cracks are formed at the same time as, or shortly after, the first cracks observed in the interior of the slabs. As a consequence of this, the smooth curvature of the slab is impaired. As the load increases, the slab becomes separated into a number of panels which are discontinuously broken up at the diagonal cracks. It is probable that these discontinuities largely reduce the torsional rigidity of the slab. It will be shown below that a close agreement with the additional deformation in tests is obtained if the torsional rigidity is put equal to zero after the development of the diagonal cracks.

⁵⁾ WÄSTLUND, G; JONSON, P. O.: Investigation on formation of cracks in reinforced concrete structure. Preliminary Publication I.A.B.S.E. 1948.

A simply supported, orthotropic, rectangular slab will now be studied more closely. Let a and b denote the sides of the slab. For an uniformly distributed load q , the deflection δ_{max} at the centre of the slab can be written ⁶⁾

$$\delta_{max} = \frac{16q}{\pi^6} \sum_{m=1,3,5..}^{\infty} \sum_{n=1,3,5..}^{\infty} \frac{(-1)^{\frac{m+n}{2}-1}}{mn \left(\frac{m^4}{a^4} D_a + \frac{2m^2 n^2}{a^2 b^2} K + \frac{n^4}{b^4} D_b \right)} \quad (33)$$

where D_a and D_b denote the rigidity of the slab in the directions a and b respectively, and K designates the torsional rigidity.

For an isotropic slab, we have

$$D_a = D_b = K = \frac{EH^3}{12(1-\nu^2)}$$

The torsional rigidity of the slab after the formation of cracks is assumed to be zero, that is to say,

$$K = 0$$

For an isotropic slab, just as for an orthotropic slab, in which $D_a = D_b$ and $K = 0$. Eq. (33) can be written

$$\delta_{max} = r \frac{q b^2}{EH^3} \quad (34)$$

For a square isotropic slab ($\nu = 0$), we have $r = 0.047$; for a square orthotropic slab, in which $D_a = D_b$ and $K = 0$, we have $r = 0.094$. It is thus seen that the deflection of a square slab is doubled when the torsional rigidity becomes equal to zero. As the ratio of the side lengths increases, the importance of the torsional rigidity becomes smaller.

The typical shape of the deflection curves obtained from tests on freely supported slabs is the same as in the case of beams, cf. Fig. 6. When the torsional rigidity is equal to zero, the additional deflections after the development of cracks, or the slope of the line Ib in Fig. 6, can be calculated from Eq. (34) if E is put equal to $E_{i,d}$ computed in the same manner as in the case of beams, and if r is chosen for $K = 0$. A comparison has been made with test results published in the literature^{2) 7) 8)}. In these calculations, the flexural rigidity was assumed to be equal in both directions, and the amount of reinforcement was expressed by its mean value for each slab. This is an approximation, but it is negligible. In some cases, the calculation of the ratio of reinforcement was slightly uncertain.

⁶⁾ HUBER, M. T.: Probleme der Statik technisch wichtiger orthotroper Platten. Warszawa 1929.

⁷⁾ BACH, C; GRAF, O.: Versuche mit allseitig aufliegenden, quadratischen und rechteckigen Eisenbetonplatten. D.A.f.E.H. 30. Berlin 1915.

⁸⁾ GEHLER, W.; AMOS, H.; BERGSTRESSER, M.: Versuche mit kreuzweise bewehrten Platten. D.A.f.E.H. 30. Berlin 1932.

Table 3. Values of the tangential modulus of elasticity obtained from the tests and calculated for concrete slabs after formation of cracks. All slabs freely supported at the edges, and were submitted to uniformly distributed loads (a and b = spans)

	No.	$a \times b$ $m \times m$	h_{av} cm	H cm	μ_{av}	$E_{test.}$ kg/cm ²	$E_{cal.}$ kg/cm ²	$\frac{E_{test.}}{E_{cal.}}$
BACH, GRAF ⁷⁾	819, 822, 824	3 × 3	6,3	8	0,0065	49000	48000	0,98
	831, 837, 840	3 × 3	10,3	12	0,0041	44000	40000	0,91
	828, 830, 841	3 × 3	6,3	8	0,0069	52000	53000	1,02
	846, 847	3 × 3	10,3	12	0,0033	37000	34000	0,92
	842, 843	3 × 3	6,3	8	0,0056	43000	48000	1,12
	884, 892, 899	3 × 3	10,0	12	0,0081	71000	68000	0,96
GEHLER ⁸⁾	1	3 × 3	10,3	12	0,0040	43000	42000	0,98
	2	3 × 3	8,3	10	0,0057	53000	52000	0,98
	2a	3 × 3	8,3	10	0,0060	55000	49000	0,89
	3	3 × 3	10,3	12	0,0040	43000	42000	0,98
	4	3 × 3	10,2	12	0,0052	55000	56000	0,98
	6	3 × 3	10,3	12	0,0040	44000	43000	0,98
NYLANDER ²⁾	Ia	3 × 3	8,4	10	0,0048	48000	46000	0,96
	Ib	3 × 3	8,4	10	0,0054	53000	48000	0,91
	Ic	3 × 3	8,4	10	0,0063	60000	57000	0,95
Av: 0,98								

The results of this comparison are reproduced in Table 3. This table gives values of the idealised modulus of elasticity observed in the tests and obtained from the calculations. On an average, the ratio of these values is equal to 0.98. If the torsional rigidity of the slabs had been unimpaired, this ratio would have been equal to 0.5. In spite of the somewhat uncertain calculations, and in spite of the influence of some other factors, e. g. the time of loading, the assumption made in the above that the torsional rigidity of the slabs decreases to zero after the development of the diagonal cracks is shown to be correct by the close agreement.

Slabs provided with torsional reinforcement at the corners exhibit a slight tendency to preserve a certain torsional rigidity, but it is, as a rule, negligible. The comparison made in the above applies to freely supported slabs only. A comparison with the results of the small number of tests made on slabs clamped at the edges shows that a corresponding reduction in rigidity takes place after the formation of cracks between the supports. Therefore, since the theoretical presuppositions are similar, the above assumptions can probably be regarded as applicable to this type of slabs too.

The decrease of the torsional rigidity to zero accounts for the rapid increase in deflection which occurs after the development of cracks between the supports.

In order to be able to determine the total deformation, we must also know the point of intersection of the line Ib and the axis of ordinates in Fig. 6, or

the coefficient γ in Eq. (22). We obtain a value on the safe side if we use the same value of γ as for beams. In reality, we obtain a slightly greater value. This is probably due to a certain slab effect remaining in the separate portions of the slab which are bounded by the supports and the diagonal cracks. For this reason, the horizontal line obtained at small ratios of reinforcement immediately after the development of cracks in beams (see Fig. 6) becomes smaller or disappears altogether. As a rule, if the ratio of reinforcement is small, we can therefore approximately assume that the two deformation lines intersect when $M = M_f$.

To sum up, it follows that, in determining the additional deformations of concrete slabs, the torsional rigidity of the slabs can be considered to be completely reduced to zero after the development of the diagonal cracks. The additional deformations after the formation of cracks can therefore be determined in the same manner as in the case of a beam frame having no torsional rigidity. The coefficient γ shall be determined as in the above.

Long-Time Loads — Their Effects on Deformations and Moment Distribution

In the design of concrete structures it is often of special interest to know the deformation and the moment distribution under the action of long-time loads. However, the factors involved are so many that this problem is difficult to solve, and the results are uncertain. In this section we propose to deal with the most important factors and to estimate their effects, partly on the basis of tests. In the first place, we shall study beams, but the results obtained in this case can, as a rule, be applied to other types of structures too.

Plastic Flow

In the case of normal stresses, the above assumptions regarding the rectilinear stress distribution can also be considered to hold good under the action of long-time loads. The reason is that the plastic flow under the stresses which are less than about 0,40 or likely more of the ultimate stress can be regarded as approximately proportional to the stress. Plastic flow lowers the position of the neutral axis, with the result that some portions of the structure which have formerly been submitted to tension are subjected to compression. This produces a slight change in the conditions for the proportionality of the plastic flow to the stress, but the resulting error is negligible. Even if the limit of proportionality is exceeded in the uppermost layer of the beam, this does not produce any notable effect on the final result. The fact that the plastic flow is proportional to the stress implies that the effective modulus of elasticity will be the same in all parts of a structure subjected to a long-time load. For instance, the flexural rigidity of a beam of constant depth at a fixed support will be the same as between the supports, even if the stress at the support is

higher. For the same reason, if a beam is cracked on the side in tension, the ratio of the flexural rigidities at the supports and between the supports will remain approximately unchanged.

Since the plastic flow of concrete under normal stresses does not produce any change in the relation between the flexural rigidities of the different parts of a structure, it will not cause any change in the moment distribution in a statically indeterminate structure. On the other hand, the deflections will increase because the effective modulus of elasticity of the concrete becomes smaller. The deflections can be calculated by inserting the smaller value of the modulus of elasticity of the concrete in the above equations.

Shrinkage

A deflection is caused by the difference in shrinkage at the top and the bottom of the beam. Prior to the formation of cracks in a beam provided with reinforcement at the bottom, the deformations due to shrinkage at the bottom of the beam are smaller owing to the counteractive effect of the reinforcement. The segregation of coarse aggregate acts in the same direction. As a rule, the influence of segregation is predominant when use is made of those concrete mixes and methods of placement which are commonly employed at the present time²). If the beam is clamped at the supports, the effect of the reinforcement at the top is favourable, but the influence of the reinforcement between the supports and the effect of segregation are normally preponderant. If the shrinkage at the top and the bottom of the beam is known, the deflection can be calculated. If the beam is clamped at the supports, the moments at the supports will change. Usually, they will increase.

When the beam is cracked on the side in tension, the number of cracks normally increases with time. This is due to two causes, viz., first, the shrinkage, and second, the fact that the strength of the concrete under the action of long-time loads is lower than the static short-time strength. Consequently, the above assumption that the concrete in the middle between two cracks is approximately stressed up to its tensile strength in bending can also be regarded as applicable under long-time loads. Accordingly, it is not necessary to take into account such factors as the plastic flow of the concrete in tension or the creep between the reinforcement and the concrete. On the other hand, the above equations must take into account the circumstance that a lower value is obtained for σ_{uf} . Some investigations indicate that the long-time strength can become as low as 50 per cent of the short-time strength. Fig. 8 ($E_c = 42,000 \text{ kg/cm}^2$) shows that the influence of the concrete in tension on the deformations under long-time loads is relatively slight.

It follows from the above that the shrinkage of a beam after the formation of cracks can be supposed not to affect the average strain of the reinforcement. During shrinkage, the tensile stress in the concrete becomes greater, with the

result that new cracks are formed. At the same time, the mean strain goes back to its previous value, which can be regarded as independent of shrinkage. As a rule, the cracks due to shrinkage are not so deep as to reach the neutral axis, but this can be disregarded. We can therefore approximately assume that the shrinkage in a beam which is cracked on the side in tension influences the deformations only on the side in compression. If the beam is cracked on the side in tension both at positive and at negative moments, the mean difference in shrinkage $\Delta \epsilon_{sh}$ between the top surface and the bottom surface can be calculated from the formula

$$\Delta \epsilon_{sh} = \frac{a \epsilon_{sh-0} - b \epsilon_{sh-u}}{l} \quad (35a)$$

where a and b are the lengths of the regions of positive and negative moment respectively, l is the span of the beam between supports, ϵ_{sh-0} and ϵ_{sh-u} are the amounts of shrinkage on the side in compression at the top and at the bottom of the beam respectively. When ϵ_{sh-0} and ϵ_{sh-u} can be assumed to be of the same size, Eq. (35a) can approximately be written

$$\Delta \epsilon_{sh} \approx \frac{a-b}{l} \epsilon_{sh} \quad (35b)$$

where ϵ_{sh} is the shrinkage of the homogeneous concrete.

On the basis of the above we can calculate the deflection. If the beam is clamped, a change will be produced in the moment at the support. As the regions of positive moment are usually longer than the regions of negative moment, the moments at the supports will increase. The magnitude of the change in the moments at the supports can be calculated by means of the usual method taking into account the angular changes. In accurate calculations it is necessary to take into account the fact that the stress distribution over the cross section is normally not linear on account of shrinkage. For approximate calculations, however, the stress distribution can be assumed to be linear. A change in the ratio of reinforcement at the supports and between the supports influences the effect of shrinkage only in so far as the resulting change in the moment distribution affects the regions of positive and negative moments. The influence of this change can generally be disregarded. Here, just as below, we assume that the yield point of the reinforcement is not reached.

Thus, shrinkage normally increases the deflection of beams with and without cracks on the side in tension, just as it normally increases the moments at the supports of clamped beams.

Ratio of Amounts of Reinforcement at Supports and between Supports

The ratio of the amounts of reinforcement at the supports and between the supports, and its influence on the deformations and the moment distribution, are of importance in the limit design of beams. In this method of

design, any arbitrary deviation of the placement of reinforcement from the distribution corresponding to the theory of elasticity is permissible on condition that the ultimate moment is constant.

Under the action of long-time loads, cracks are generally formed on the sides in tension. In that case the flexural rigidity is dependent on the amount of reinforcement. If the beam is clamped at the supports, the ratio of the flexural rigidities at the supports and between the supports after the development of cracks may differ from the corresponding ratio before the formation of cracks. This causes a transfer of moments. Accordingly, the moments at the supports can be increased or reduced by varying the ratio of the amounts of reinforcement at the supports and between the supports. In addition, the deflection will be dependent on this variation.

We shall now make a more detailed study of the relation between the moment at a support and the deformation, on the one hand, and the ratio of the amounts of reinforcement at the supports and between the supports, on the other hand, in the case of a beam of rectangular cross section clamped at both supports and subjected to a uniformly distributed load. We assume that cracks have formed on the side in tension both at the supports and between the supports. Those beams in which cracks have developed at the supports only are regarded as an intermediate type, and will be disregarded in what follows. (In such beams, a decrease in the amount of reinforcement at the supports causes a slight reduction in the moments at the supports and a slight increase in the deflection. If the amount of reinforcement determined in accordance with the theory of elasticity is reduced to a half, the deflection increases $\lesssim 20$ per cent.) The flexural rigidity is expressed by means of Eq. (23 b). In the following calculations we disregard the contributive effect of the concrete in tension, that is to say, we assume $M_f = \frac{b H^2}{6} \sigma_{cf} \approx 0$, and we obtain where d is a constant.

$$E J \approx \frac{b h^3}{5,0} \sqrt{\mu E_s E_c} = d \sqrt{\mu} \quad (36)$$

In order to ensure the same safety against failure throughout the structure, the sum of the moments at the supports and between the supports shall be constant. This implies that the sum of the amounts of reinforcement at the supports ($=\mu_s$) and between the supports ($=\mu_f$) can be assumed to be approximately constant ($=\mu_\epsilon$).

Thus, we obtain

$$\mu_s + \mu_f = \mu_\epsilon \quad (37)$$

The flexural rigidity of the parts of the beam subjected to negative and positive moments is assumed to be determined by μ_s and μ_f respectively.

On the basis of the above assumption, the variation in the moment at a support with the ratio of the amounts of reinforcement at the supports and

between the supports can be calculated by means of Eqs. (36) and (37). The result of this calculation is reproduced in Fig. 9. The deviations from the usually assumed moment at a support $\frac{1}{12}ql^2$ are relatively slight, if we except very extreme values of the ratio of reinforcement. If the ratio of reinforcement at the supports increases to 80 per cent of μ_ϵ or decreases to 20 per cent of μ_ϵ , the deviation becomes less than 15 per cent. Furthermore, it is to be noted that the contributive effect of the concrete in tension has been disregarded in these calculations, and this has an unfavourable influence on the results. The

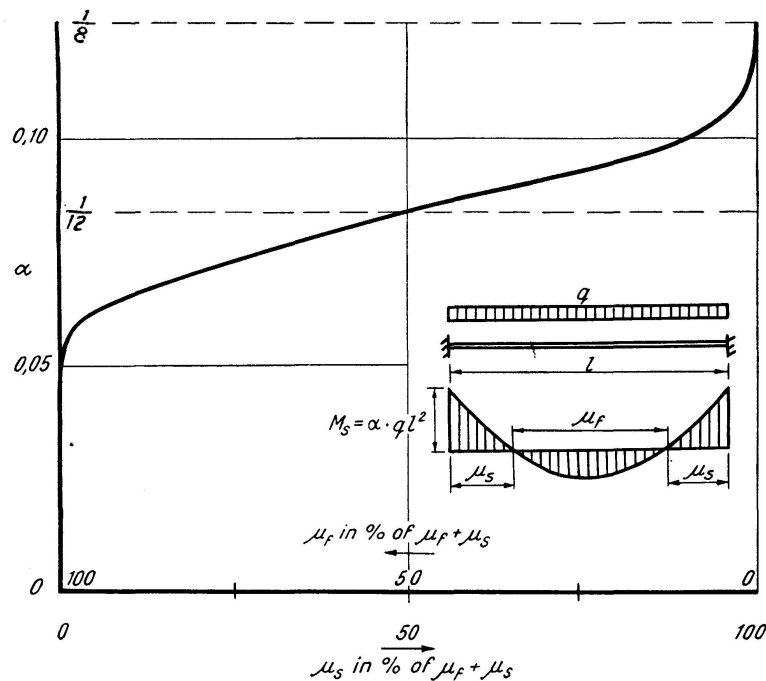


Fig. 9. Calculated variation in the moment at the support with the distribution of reinforcement at the supports and between the supports (μ = ratio of reinforcement)

actual moment will be comprised between the theoretically calculated curve in Fig. 9 and $\frac{1}{12}ql^2$. Moreover, the actual value of the moment at a support includes its change, usually an increase, due to non-uniform shrinkage. It is of interest to observe that the common method of designing reinforcement in accordance with the theory of elasticity, $\mu_s \approx 0.67\mu_\epsilon$, results in a moment at a support which is slightly greater than that serving as a basis for the design of reinforcement.

The variation in the deflection with the ratio of reinforcement is of great interest. The result of the calculations is reproduced in Fig. 10. This result is remarkable. It shows that the deflection within a very wide interval is nearly independent of the ratio of the amounts of reinforcement at the supports and between the supports. For instance, if the ratio of reinforcement at the supports decreases to 30 per cent of μ_ϵ or increases to 80 per cent of μ_ϵ , the cor-

responding increase in deflection does not exceed a few per cent. Furthermore, it is to be noted that the above approximation $M_f \approx 0$, which disregards the contributive effect of the concrete in tension, has an unfavourable influence at the extreme values of the ratio of reinforcement. If the concrete in tension were taken into account, the variations in deflection would therefore be still smaller.

In spite of the relatively schematic assumptions made for the above calculations, we can draw the conclusion that the deflections within a relatively wide interval are nearly independent of the ratio of the amounts of rein-

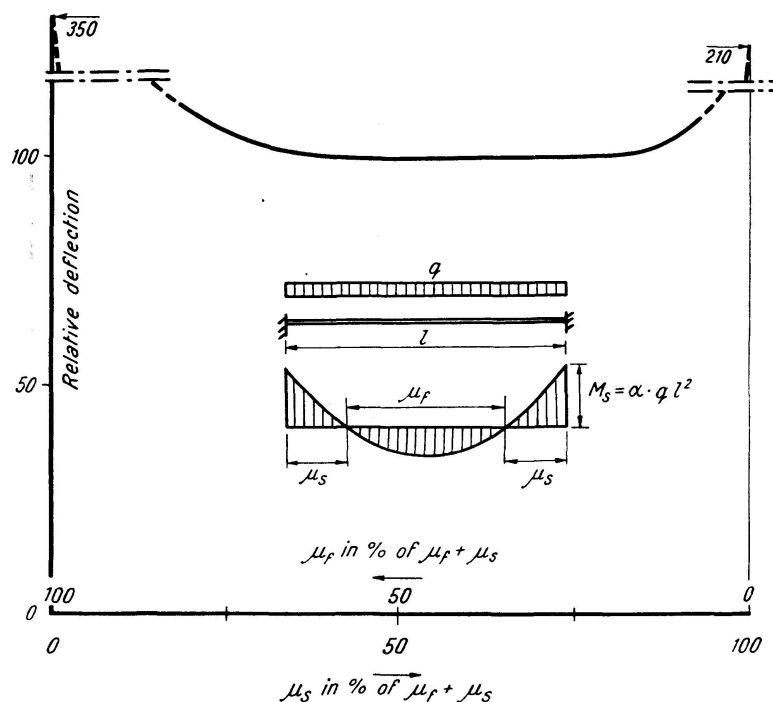


Fig. 10. Calculated variation in deflection with the distribution of reinforcement at the supports and between the supports (μ = ratio of reinforcement)

forcement at the supports and between the supports even after the development of cracks in the beam. These calculations take no account of shrinkage and plastic flow. However, it follows from the above that the deflection due to shrinkage can be regarded as independent of the ratio of reinforcement after the formation of cracks in a beam. As a rule, this statement is also applicable prior to the development of cracks. The deflection due to plastic flow is also relatively independent of the ratio of reinforcement. The increase of the compressive stress in the concrete which would be obtained if, for instance, the ratio of reinforcement at the supports were reduced to a half is not so great (about 30 per cent) as to cause the stress at normal loads to reach that value at which the proportionality of the plastic flow to the stress is exceeded.

To sum up, we can state, on the basis of the above theoretical assumptions, that when a beam is fixed at both supports and subjected to a uniformly

distributed load, the deflection is approximately independent of the ratio of the amounts of reinforcement at the supports and between the supports within a wide interval ($0.30 \mu_\epsilon \lesssim \mu_s \lesssim 0.80 \mu_\epsilon$). A corresponding result is obtained under other conditions at the supports. The results obtained in the above ought to be applicable to other types of structures too, e. g. slabs. As has been shown in the above, after the development of the diagonal cracks, the structural action of slabs can be considered to be largely similar to that of beam frames having no torsional rigidity.

Conclusions for Design

The choice of a suitable ratio of the amounts of reinforcement at the supports and between the supports is a question of engineering economy. However, if the cost remains the same irrespective of whether the reinforcement is placed at the supports or between the supports, then the reinforcement shall be designed in accordance with the real moment distribution. This results in optimum economical structures both as regards the ultimate strength and in respect of deformations. As the load increases, the yield point is reached simultaneously at the supports and between the supports, and approximately at the same time as the load reaches its ultimate value. On the other hand, if, e. g. the amount of reinforcement at the supports is reduced in favour of the reinforcement between the supports, then the yield point will first be reached, and harmful deformations will therefore usually be produced, at a support before the load has reached its ultimate value, and this is unfavourable. In some cases, however, it is cheaper to reduce the amount of reinforcement at the supports in favour of the reinforcement between the supports. This saving must be weighed against the slight inadequacy of the structure under heavy loads. On the other hand, if the probability of loads which are so heavy that the yield point can be reached at a support is negligible even after a reduction in the amount of reinforcement at the support, then it follows from the above that the structures will be approximately equivalent also in respect of deformations.

Under normal loads, as has previously been shown, the actual moment distribution is in relatively close agreement with the moment distribution calculated for a homogeneous cross section in conformity with the theory of elasticity. Nevertheless, the moments can be subject to corrections due to non-uniform shrinkage. This moment distribution remains fairly correct also when the load approaches its ultimate value, at least in under-reinforced beams, as will also be seen from the tests described in what follows. *A moment distribution in accordance with the real which is usual closely in agreement with the theory of elasticity should therefore be chosen as a basis for design. A departure from this distribution can be justified by an economic comparison.* For an accurate determination of the ultimate load it is advisable to use a calculation based on

the limit design method, particularly when dealing with those structures which are to a high degree statically indeterminate, e. g. slabs (see K. W. JOHANSEN).

Tests

In order to verify the theoretical results obtained in the above, the Author has made long-time tests on beams at the Division of Building Statics and Structural Engineering, the Royal Institute of Technology, Stockholm, in 1948. The test series comprised three beams. All these beams were fixed at both supports. The beams were subjected to the action of their own weight and to concentrated loads at $1/3$ points of span. This method of loading is close to a uniformly distributed load. The ratio and the moments at the supports and between the supports is the same in these two cases, and the shapes of the moment diagrams are relatively similar. Two of the beams were constant in depth, while the third beam was provided with small V-shaped projections at the supports. The reinforcement of the beam with projections and of one of the beams of constant depth was designed in accordance with the theory of elasticity. The reinforcement of the third beam considerably differed from that corresponding to the theory of elasticity in that the reinforcement at the supports was reduced to a half ($\mu_s = 0.33 \mu_e$) and the reinforcement between the supports was doubled ($\mu_f = 0.67 \mu_e$). In other words, the reinforcement

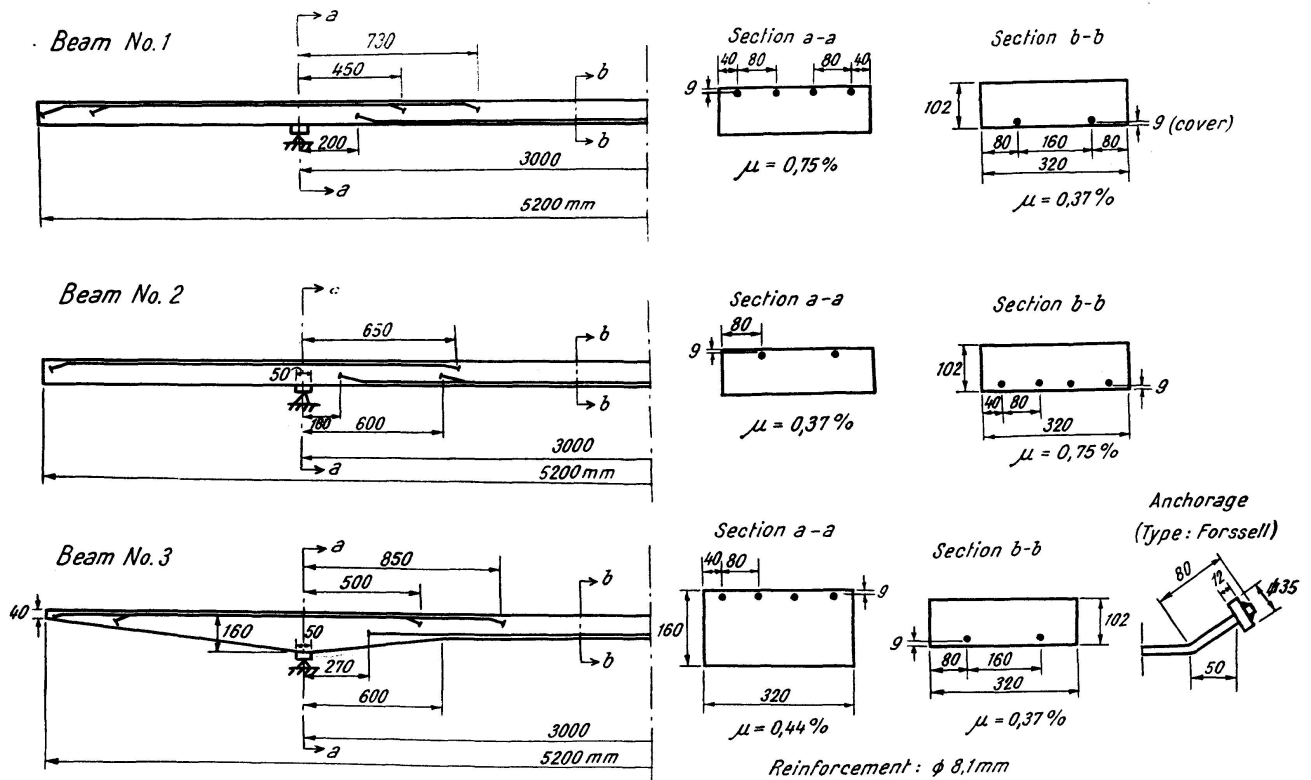


Fig. 11. Dimensions and reinforcement of the beams subjected to the tests

required between the supports according to the theory of elasticity was placed at the supports, whereas the corresponding reinforcement at the supports was placed between the supports.

The dimensions and the reinforcement of the beams subjected to the tests are shown in Fig. 11.

The concrete mix used for the beams had the proportion cement: fine aggregate: coarse aggregate = 1:4.5:6.75. The water-cement ratio was 0.88. The consistency was 5 to 7 degrees VB.

Nine cubes for compressive tests were made at the same time as each beam. The results of the check tests are given in Table 4. The steel used for the beam reinforcement had a yield point stress of 4280 kg/cm².

All test specimens were cured under wet sacks up to the testing day (the beams were cured 28 days). After that, the specimens for the long-time tests were stored in a room where the temperature was 16 to 19°C and the relative moisture content was 50 to 60 per cent.

Table 4. Results of check tests, and the stresses due to long-time loads calculated in accordance with the theory of elasticity ($n = 15$)

Beam No.	Compression strength of cubes (Sidlength = 15 cm) ⁹⁾ kg/cm ²						Age days
1	276, 271, 263, 264, 269, 265			Av: 268			29
	354, 348, 335			Av: 346			250
2	275, 283, 262, 279, 276, 282			Av: 276			28
	392, 396, 378			Av: 389			245
3	295, 277, 257, 286, 286, 297			Av: 283			30
	363, 369, 336			Av: 356			265
Calculated stresses							
Support				Mid-span			
	$\sigma_{cf}^{10)$ $\left(= \frac{6M}{bh^2} \right)$ kg/cm ²	$\sigma_s^{11)$ kg/cm ²	$\sigma_c^{11)$ kg/cm ²	$\sigma_{cf}^{10)$ $\left(= \frac{6M}{bh^2} \right)$ kg/cm ²	$\sigma_s^{11)$ kg/cm ²	σ_c kg/cm ²	
1	39	1300	52	19	1270	34	
2	39	2550	68	19	640	26	
3	29	1420	42	8	1270	34	

⁹⁾ Cubes compressed between steel plates.

¹⁰⁾ Non-cracked beam (Stage I).

¹¹⁾ Cracked beam (Stage II).

In order to secure fixed clamping at the supports, a water level was used to make sure that the change in angle was equal to zero. The accuracy in water level readings was $1.5 \cdot 10^{-5}$ radians. This corresponded to a measurable difference of 0.5 kgm in the moments at the supports. Two water levels were embedded in concrete on the side in compression at each support. When this method of measurement was used in the check tests, it was found to be reliable also after the development of small cracks. At large deformations under the ultimate load, the fixed clamping was checked by means of dial gauges.

The beams were insulated by a coating of lacquer on the sides, so as to ensure that the concrete should be dried on the top and bottom surfaces only. The deflection at the centre of the beam with respect to the supports was measured by means of dial gauges.

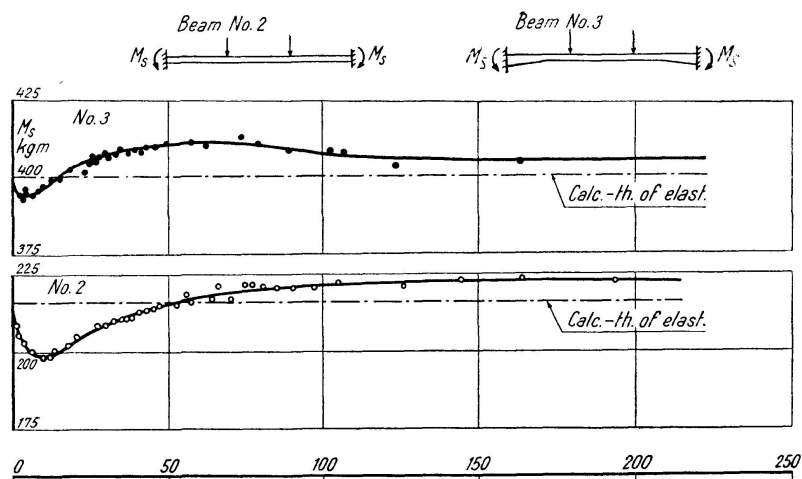


Fig. 12. Variation in the moments at the supports with the duration of the loading period

In the long-time tests, the loads at $1/3$ points of span were 235 kg on the beams Nos. 1 and 2, and 422 kg on the beam No. 3. The magnitude of the loads was adjusted so as to produce in the beams Nos. 1 and 3, both at the supports and between the supports, a stress in steel of about 1300 kg/cm^2 calculated in accordance with the Swedish standard specifications ($n = 15$). The stresses due to the long-time loads are given in Table 4.

The moment distribution observed on all test beams after the application of the load was closely similar to that calculated from the theory of elasticity. The variations in the moments at the supports with the duration of the loading period are represented in Fig. 12. The wide variations observed during the first days can probably be attributed to the differences in the moisture content in the layers of concrete in the immediate neighbourhood of the top and bottom surfaces of the beams due to the method of curing. The measuring devices at one of the supports of the beam No. 1 were slightly damaged. For this reason, the observed moments at the supports are somewhat smaller, and

the deflections are slightly greater, than their actual values. The results of the long-time test on this beam have therefore been omitted in Fig. 12.

It is seen from the test results that the moments at the supports of the beams Nos. 2 and 3 after some time become greater than the values computed in accordance with the theory of elasticity. This is mostly due to the shrinkage of the concrete, as has already been mentioned. Furthermore, the moment distribution is influenced by the development of cracks, which has after some time been observed on these two beams both at the supports and between the supports. However, this tendency cannot be clearly distinguished in the test results because the influence of shrinkage is greater.

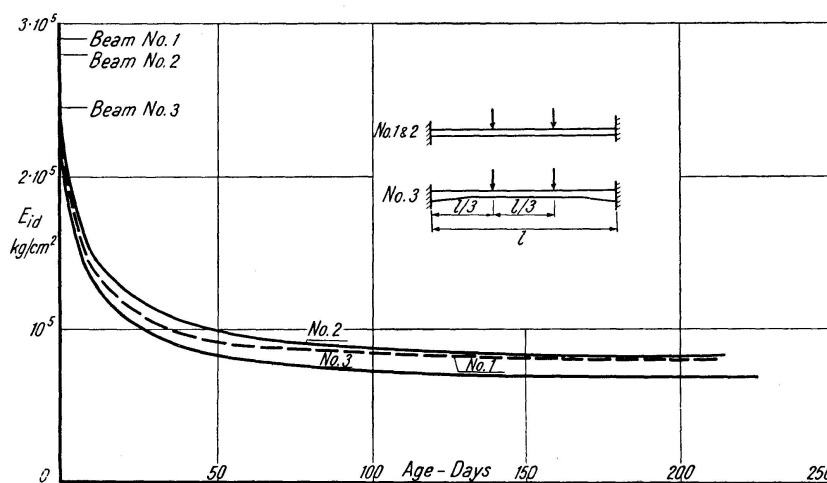


Fig. 13. Variation in the idealised modulus of elasticity with the duration of the loading period

Fig. 13 shows how the idealised moduli of elasticity calculated from the deflections vary with the duration of the loading period. The curve for the beam No. 1 has been corrected for the above-mentioned error in measurements. The uncertainty in the observed values due to this correction is probably less than about 2 per cent. It is seen from the diagram that the moduli of elasticity rapidly decrease in the beginning and then approach a limiting value. The rapid decrease of the rigidity at the outset is largely due to the formation of cracks, which was greatest during the first part of the loading period. After 215 days, the moduli of elasticity decreased to the following values, viz., 81,000 kg/cm² for the beam No. 1, 82,000 kg/cm² for the beam No. 2, and 68,000 kg/cm² for the beam No. 3. The beam No. 3 shall have a smaller idealised modulus of elasticity on account of the lower mean ratio of reinforcement. The relative deflections are given in Table 5. The deflection of the beam No. 3 has been reduced so as to correspond to the deflection of a beam having the same depth and the same mean ratio of reinforcement as the beams Nos. 1 and 2. It is seen from Table 5 that the values are closely in agreement. Consequently, the test confirm our statement that even a large deviation from

the distribution of reinforcement at the supports and between the supports determined in accordance with the theory of elasticity does not produce any notable influence on the deflection, a statement which has previously been based on calculations.

Table 5. Comparison of the deflections observed in tests after 215 days. (The deflection of beam No. 3 has been transformed to be equivalent with beams like No. 1 and 2)

Beam No.	Relative deflections
1	100
2	99
3	104

After the long-time tests, the load applied to the beams was increased until failure was produced. The moments and the deflections were measured at the ultimate load. The moment distribution observed at the ultimate load is represented in Fig. 14. Since the clamping of the beams at the ultimate load

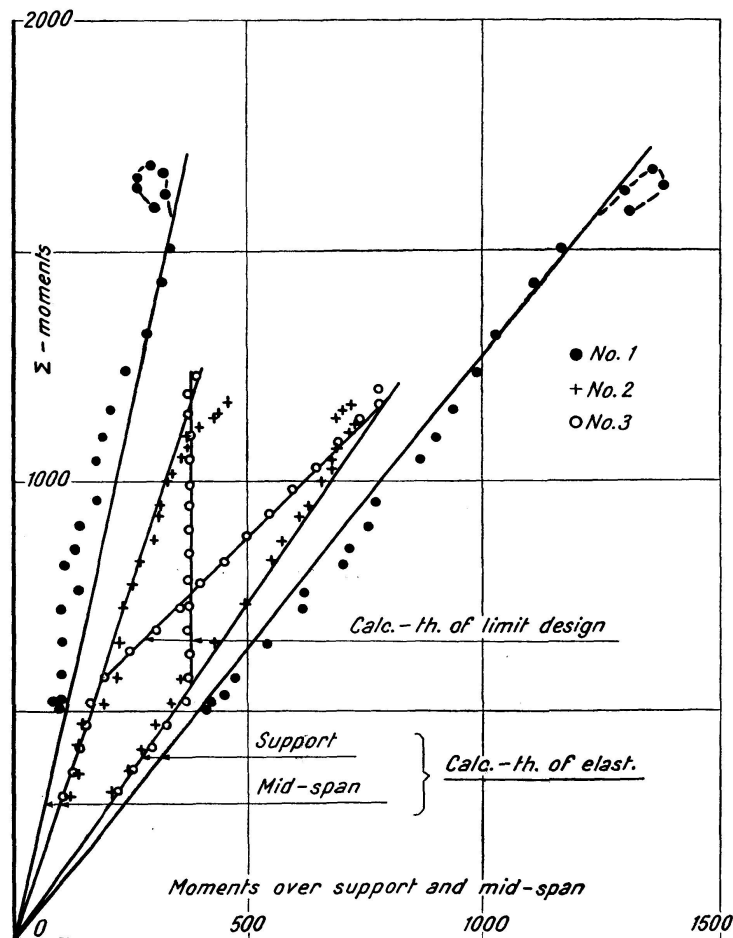


Fig. 14. Moment distribution observed at the ultimate load

was checked by means of a less accurate method of measurement, it was not possible to make accurate measurements of the transfer of moments caused by the development of cracks and amounting to a few per cent. The moment acting on the beam No. 2 adjusted itself to the reinforcement after the yield point had been reached at the supports.

The loading of the beams was continued also after the yield point had been exceeded. The loads were slightly increased as the deflection became greater. As an example, Fig. 15 shows the moments plotted against the deflection of the beam No. 3. Failure took place when the deflection was as large as 29.5 cm. It occurred in shear. Thus, at the ultimate load, the slope of the beam between the point of load application and a support was about 1:3. The tests demonstrate the great deformability, and hence the great load-bearing capacity, of under-reinforced beams.

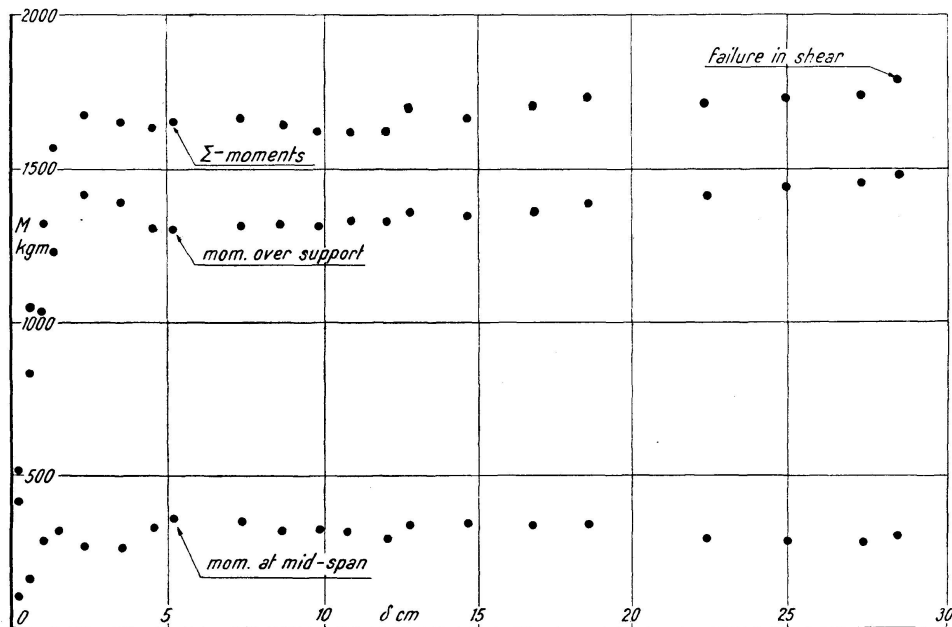


Fig. 15. Moments plotted against the deflection of the test beam No. 3 at the ultimate load

The test results were in close agreement with the values computed by means of the limit design method. The respective values of the moments, in kgm, at the beginning of yield were as follows: 1170 and 1160 for the beam No. 1, 1140 and 1160 for the beam No. 2, and 1580 and 1660 for the beam No. 3.

Acknowledgements

The investigation described in this paper has been carried out at the Division of Building Statics and Structural Engineering, the Royal Institute of Technology, Stockholm, and the Author wishes to express his deep gratitude to the Director of the Division, Professor HENRIK NYLANDER.

Summary

The deformations of reinforced concrete are studied in this paper on the basis of the mechanical properties of materials, at loads which are not in the neighbourhood of the ultimate load. The amount of reinforcement and the contributive effect of the concrete in tension are taken into account also after the development of cracks. Prisms, beams, and slabs are dealt with, and comparisons are made between theoretical and experimental results.

It is demonstrated that the deformations of a reinforced concrete structure after the development of cracks can be written in the general form

$$\delta = \delta_{II} - \Delta \delta$$

where δ_{II} denotes the deformations calculated in accordance with the classical theory, which disregards the concrete in tension, and $\Delta \delta$ expresses the influence of the contributive effect of the concrete in tension between the cracks, which is constant and independent of the total strain of the tensile reinforcement, as long as the bond between the reinforcement and the concrete is not impaired, e. g. by alternate loads. Since $\Delta \delta$ is dependent on the method of loading, it is, as a rule, difficult to determine the actual deformations in advance with a sufficient degree of accuracy. On the other hand, it is possible to calculate two limits, viz., a lower limit corresponding to the full contributive effect of the concrete in tension ($=\delta_{II} - \Delta \delta$), and an upper limit ($=\delta_{II}$) corresponding to the complete absence of this contributive effect.

Equations are deduced for calculating the elongation of the reinforcement, the compression of the concrete, the position and the displacements of the neutral layer, the flexural rigidity, and hence the deflection, the distance between cracks, and the widths of cracks.

It is shown that reinforced concrete slabs after the formation of cracks in the interior of the slabs can be regarded as devoid of torsional rigidity.

The effects of plastic flow and shrinkage are studied under long-time loading. Furthermore, it is demonstrated that even a relatively large deviation from the reinforcement designed in accordance with the theory of elasticity in statically indeterminate structures produces but a slight effect on the magnitude of the deflection and on the moment distribution under the action of long-time loading. This statement is based on the assumption that the total amount of reinforcement is constant and that the yield point is not exceeded.

Zusammenfassung

Die vorliegende Untersuchung der Formänderungen des Eisenbetons stützt sich auf die Festigkeitseigenschaften der Werkstoffe bei Belastungen, die nicht in der Nähe der Bruchlasten liegen. Die Bewehrungsmenge und die Mitwirkung des auf Zug beanspruchten Betons werden auch nach der Reiß-

bildung berücksichtigt. Prismen, Balken und Platten werden behandelt, wobei Versuchsergebnisse zum Vergleich mit der Theorie herangezogen werden.

Es wird bewiesen, daß die Formänderungen einer Eisenbetonkonstruktion nach der Rißbildung sich in der allgemeinen Form

$$\delta = \delta_{II} - \Delta \delta$$

ausdrücken lassen. Dabei bezeichnet δ_{II} die nach der klassischen Theorie ohne Berücksichtigung des auf Zug beanspruchten Betons berechneten Formänderungen und $\Delta \delta$ ist der Einfluß der Mitwirkung des auf Zug beanspruchten Betons zwischen den Rissen, der konstant und von der Gesamtdehnung der Zugbewehrung unabhängig ist, solange die Haftkraft zwischen dem Beton und der Bewehrung, z. B. durch Wechselbelastung, nicht beeinträchtigt wird. Da $\Delta \delta$ von der Belastungsweise abhängig ist, sind die tatsächlichen Formänderungen schwer im voraus genau zu bestimmen. Dagegen kann man zwei Grenzen angeben, und zwar die untere Grenze, die der vollen Mitwirkung des auf Zug beanspruchten Betons entspricht ($= \delta_{II} - \Delta \delta$) und die obere Grenze ($= \delta_{II}$), die dem vollständigen Aufhören dieser Mitwirkung entspricht.

Gleichungen werden aufgestellt für die Berechnung der Dehnung der Bewehrung, der Zusammendrückung des Betons, der Lage und der Verschiebungen der Nullschicht, der Biegesteifigkeit, und somit der Durchbiegung, des Abstandes zwischen den Rissen und der Rißbreite.

Es wird gezeigt, daß Eisenbetonplatten nach der Rißbildung in den inneren Teilen der Platte ihre Verdrehungssteifigkeit so gut wie völlig verlieren.

Der Verfasser untersucht die Einflüsse beim Plastischwerden und bei der Schrumpfung des Betons bei Dauerlasten. Er beweist ferner, daß auch eine verhältnismäßig starke Abweichung von der nach der Elastizitätstheorie berechneten Bewehrung in statisch unbestimmten Konstruktionen die Größe der Durchbiegung und die Momentverteilung bei Dauerlasten nur wenig beeinflußt. Dabei wird vorausgesetzt, daß die Bewehrungsmenge konstant ist und die Streckgrenze nicht überschritten wird.

Résumé

Les déformations du béton armé sont étudiées dans ce rapport sur la base des propriétés mécaniques des matériaux à des charges qui ne sont pas au voisinage des charges de rupture. On tient compte de la quantité d'armatures et de l'effet contributif du béton soumis à la traction tant avant qu'après la fissuration. L'auteur examine les prismes, les poutres et les dalles, en faisant des comparaisons entre les résultats théoriques et expérimentaux.

Il démontre qu'on peut exprimer les déformations d'une construction en béton armé après la formation de fissures sous la forme générale

$$\delta = \delta_{II} - \Delta \delta$$

où δ_{II} désigne les déformations calculées suivant la théorie classique, qui néglige le béton soumis à la traction, alors que $\Delta \delta$ indique l'influence de l'effet contributif du béton soumis à la traction entre les fissures, influence qui est constante et indépendante de l'allongement total de l'armature de traction, tant que l'adhésion du béton aux armatures n'est pas endommagée, par ex. sous l'action des charges alternatives. Puisque $\Delta \delta$ dépend de la méthode d'application de la charge, il est généralement difficile de déterminer d'avance les déformations réelles d'une manière précise. D'autre part, on peut calculer deux limites, à savoir: une limite inférieure qui correspond à l'effet contributif tout entier du béton soumis à la traction ($= \delta_{II} - \Delta \delta$) et une limite supérieure ($= \delta_{II}$) qui correspond à l'absence complète de cet effet contributif.

L'auteur déduit des équations qui servent à calculer l'allongement des armatures, la compression du béton, la position et les déplacements de la couche neutre, la rigidité de flexion, et partant la flèche, la distance entre les fissures et la largeur des fissures.

Il montre que les dalles en béton armé peuvent être considérées comme étant dépourvues de rigidité de torsion après la formation de fissures dans la partie intérieure de la dalle.

Les effets de la transition à l'état plastique et du rétrécissement du béton sont étudiés sous l'action des charges de longue durée. En outre, l'auteur démontre que même un écart relativement grand de l'armature calculée suivant la théorie de l'élasticité, dans les constructions hyperstatiques, ne produit qu'un effet faible sur la grandeur de la flèche et sur la distribution des moments sous l'action des charges de longue durée, dans l'hypothèse que la quantité totale d'armature soit constante et que la limite d'étirage ne soit pas dépassée.